

Published in final edited form as:

*Nano Lett.* 2011 November 9; 11(11): 4932–4938. doi:10.1021/nl2028766.

## Reactive Oxygen Species Driven Angiogenesis by Inorganic Nanorods

Chitta Ranjan Patra<sup>1,2,\*</sup>, Jong Ho Kim<sup>3,4</sup>, Kallal Pramanik<sup>5,§</sup>, Livius V. d'Uscio<sup>6</sup>, Sujata Patra<sup>2</sup>, Krishnendu Pal<sup>2</sup>, Ramani Ramchandran<sup>5</sup>, Michael S Strano<sup>3</sup>, and Debabrata Mukhopadhyay<sup>2,7,\*</sup>

<sup>1</sup>Department of Chemical Biology, Indian Institute of Chemical Technology, Uppal Road, Tarnaka, Hyderabad - 500607, AP, INDIA

<sup>2</sup>Department of Biochemistry and Molecular Biology, 200 First Street S.W., Mayo Clinic College of Medicine, Mayo Foundation, Rochester, MN 55905, USA

<sup>3</sup>Department of Chemical Engineering, Massachusetts Institute of Technology, Cambridge, Massachusetts 02139

<sup>4</sup>Department of Chemical Engineering, Hanyang University, Ansan 426-791, Republic of Korea

<sup>5</sup>Developmental Biology Division, Developmental Vascular Biology Program, Medical College of Wisconsin and Children's Research Institute, Milwaukee, Wisconsin 53226

<sup>6</sup>Department of Anesthesiology and Molecular Pharmacology, Mayo Clinic College of Medicine, Rochester, MN 55905, USA

<sup>7</sup>Department of Biomedical Engineering, 200 First Street S.W., Mayo Clinic College of Medicine, Mayo Foundation, Rochester, MN 55905, USA

### Abstract

The exact mechanism of angiogenesis by europium hydroxide nanorods was unclear. In this study we have showed that formation of reactive oxygen species ( $H_2O_2$  and  $O_2^{\bullet-}$ ) are involved in redox signaling pathways during angiogenesis, important for cardiovascular and ischemic diseases. Here we used single-walled carbon nanotube (SWNT) sensor array to measure the single-molecule efflux of  $H_2O_2$  and a HPLC method for the determination of  $O_2^{\bullet-}$  from endothelial cells in response to pro-angiogenic factors. Additionally, ROS-mediated angiogenesis using inorganic nanorods was observed in transgenic (*flil1a:EGFP*) zebrafish embryos.

\*To whom correspondence should be addressed: Chitta Ranjan Patra, Ph.D., <sup>1</sup>Department of Chemical Biology, Indian Institute of Chemical Technology, Uppal Road, Tarnaka, Hyderabad - 500007, AP, INDIA, Tel: +91-9666204040 (Mobile), +91-40-27191809, (O), Fax: +91-40-27160387/27160757, CRPatra@iict.res.in, Additional ID: patra.chitta@gmail.com. Debabrata Mukhopadhyay, <sup>2,6</sup>Department of Biochemistry and Molecular Biology, Gugg 13-21C, Mayo Clinic College of Medicine, 200 First St. S.W., Rochester MN 55905. Tel: 507-538-3581; Fax: 507-293-1058, mukhopadhyay.debabrata@mayo.edu.  
<sup>§</sup>Current address: Prescient Life Science, New Delhi

### CONFLICT OF INTEREST STATEMENT:

Mayo Foundation for Medical Education and Research has filed a patent (Patent Application No.# PCT/US2007/075926) entitled "RARE EARTH NANOPARTICLES" which lists Drs. Chittaranjan Patra, and Debabrata Mukhopadhyay as inventors. Dr. Patra and Dr. Mukhopadhyay disclosed that they and Mayo Clinic have a financial interest in the technology related to this research. That technology has been licensed to a privately held biotechnology company. Mayo Clinic holds equity in this company, and Mayo Clinic and Drs. Patra and Mukhopadhyay have contractual rights to receive future royalties from the licensing of this technology.

Supporting Information Available: Materials, methods, experimental techniques etc. have been described in supporting information. This material is available free of charge via the Internet at <http://pubs.acs.org>.

## Keywords

Europium hydroxide [Eu<sup>III</sup>(OH)<sub>3</sub>] nanorods; reactive oxygen species (ROS); hydrogen peroxide (H<sub>2</sub>O<sub>2</sub>); single-walled carbon nanotubes (SWCNT); *in vivo* angiogenesis; zebrafish model

Angiogenesis is the process of formation of new capillaries from pre-existing blood vessels,<sup>1</sup>. It is a complex process, involving both pro- and anti-angiogenic factors, and plays an important role in physiological and pathophysiological processes such as embryonic development, proliferative diabetic retinopathy, atherosclerosis, post-ischemic vascularization of the myocardium, tumor growth and metastasis, and rheumatoid arthritis, etc.<sup>1a,2</sup>. However, angiogenesis has also been used to enhance blood flow through collateral blood vessels in patients with cardiovascular diseases (CVD), including ischemic heart disease (IHD), ischemic limb disease (IHD), peripheral vascular diseases, and other diseases using pro-angiogenic cytokines. Cardiovascular ischemia is the leading cause of morbidity and mortality in the Western as well as developing countries<sup>3</sup>. One therapeutic strategy for the treatment of CVD is the application of pro-angiogenic factors or cytokines, such as vascular endothelial growth factor A (VEGF-A) and basic fibroblast growth factor (bFGF)<sup>1a, 2a</sup>, to enhance blood flow in ischemic tissues via formation of collateral blood vessels<sup>2a, 4</sup>. However, this technique is associated with pathological angiogenesis, thrombosis, fibrosis, and/or the proliferation of tumor cells<sup>4a</sup>. The latter observation warrants further development of novel pro-angiogenic, as well as anti-angiogenic molecules, for treatment of ischemic diseases. For this aspect, nanotechnology may provide an alternative<sup>4c,5</sup>. Such an approach necessitates identifying novel compounds that specifically promote angiogenesis in ischemic tissues without affecting the process of angiogenesis in other tissues.

Recently, we have demonstrated that europium hydroxide [Eu<sup>III</sup>(OH)<sub>3</sub>] nanorods (inorganic nanorods) exhibit significant pro-angiogenic activities (like cytokines, such as VEGF and bFGF) and are non-toxic to *in vitro* and *in vivo* models<sup>5</sup>. Considering the huge implications of angiogenesis in CVD, it is an important area of research to develop more efficient and effective alternative treatment strategies for cardiovascular diseases (CVD) using inorganic nanorods. Hence, it is essential to understand in greater depth the molecular mechanisms and regulatory signaling pathways that explain inorganic nanorod-mediated angiogenesis. In this report, we show that the generation of reactive oxygen species (ROS) [superoxide anion (O<sub>2</sub><sup>•-</sup>) (rapidly transformed into H<sub>2</sub>O<sub>2</sub>), and hydrogen peroxide (H<sub>2</sub>O<sub>2</sub>)], especially H<sub>2</sub>O<sub>2</sub> in the presence of Eu<sup>III</sup>(OH)<sub>3</sub> nanorods regulates angiogenesis in both *in vitro* and *in vivo* models. These two ROS are the most biologically important ROS that stimulate cell migration and proliferation, tube formation, and other processes that are key steps in angiogenesis<sup>6</sup>. Accordingly, we have detected the formation of O<sub>2</sub><sup>•-</sup> by a standard HPLC method and utilized a near infrared fluorescent single-walled carbon nanotube (SWNT) sensor array to measure the single-molecule efflux of H<sub>2</sub>O<sub>2</sub> from human umbilical vein endothelial cells (HUVEC) in response to pro-angiogenic factor [Eu<sup>III</sup>(OH)<sub>3</sub>]. Finally, we have demonstrated ROS-mediated angiogenesis (in the formation of subintestinal vessels) using inorganic nanorods in transgenic (*fli1a:EGFP*) zebrafish embryos. This study may provide the basis for the future development of new alternative therapeutic treatment strategies for diseases in which angiogenesis plays a significant role such as CVD, ischemic heart, limb diseases, and cancers.

Europium hydroxide [Eu<sup>III</sup>(OH)<sub>3</sub>] nanorods were synthesized according to our earlier publication but with a modification where the molar ratio of NH<sub>4</sub>OH and europium (OH/Eu) was 4<sup>5a</sup>.



The characterization of nanorods was carried out using several physico-chemical techniques. The crystal structure of the as-synthesized product, obtained after 60 min of MW heating, was identified using XRD analysis, which indicated the crystalline nature of the product (Figure 1a). The morphologies of the as-synthesized nanomaterials were characterized with low-resolution transmission electron microscopy (LRTEM) that clearly showed that  $\text{Eu}(\text{OH})_3$  (Figure 1b) consists entirely of nanorods with a diameter of 35–50 nm and a length of 200–300 nm. For comparison purposes, we purchased europium oxide  $\text{Eu}_2\text{O}_3$  nanopowder with ~200-nm particle size from Sigma-Aldrich (USA), and its TEM image is presented in supplementary information (SI-Figure1).

After physico-chemical characterization of the nanorods, they were tested for *in vitro* functional activity in HUVEC. Cell proliferation is one of the key steps in angiogenesis; and hence, the study of pro-angiogenic properties of  $\text{Eu}^{\text{III}}(\text{OH})_3$  nanorods was carried out in HUVEC using the radioactive [ $^3\text{H}$ ]-thymidine incorporation assay <sup>5a</sup>(Figure 1c). When compared with an untreated control HUVEC, these nanorods promoted a dose-dependent increase in endothelial cell proliferation in the concentration range of 1–10  $\mu\text{g}/\text{ml}$  (Figure 1c). Maximum endothelial cell proliferation (~3.2 fold) was observed at nanorod concentrations of 5  $\mu\text{g}/\text{ml}$ , and there is almost no change of stimulation at 10  $\mu\text{g}/\text{ml}$ . VEGF stimulation was used as a positive control. These results demonstrate the capacity of  $\text{Eu}^{\text{III}}(\text{OH})_3$  nanorods to induce EC proliferation at low concentrations (5–10  $\mu\text{g}/\text{ml}$ ). Previously, we had demonstrated the pro-angiogenic properties of  $\text{Eu}^{\text{III}}(\text{OH})_3$  nanorods in several *in vitro* and *in vivo* assays (CAM: chick chorioallantoic membrane assays) <sup>5a</sup> where we used a higher concentration (20–100  $\mu\text{g}/\text{mL}$ ) of nanorods. However, in this modified method (reducing the  $\text{NH}_4\text{OH}/\text{Eu}^{3+}$  molar ratio from 40 to 4; pH 5.5), the as-synthesized nanorods show better EC proliferative activity at low concentrations.

In order to compare the EC proliferative activities of our microwave-assisted as-synthesized  $\text{Eu}^{\text{III}}(\text{OH})_3$  nanorods with commercially available  $\text{Eu}_2\text{O}_3$  nanopowders, we also carried out a dose-dependent cell proliferation assay with these  $\text{Eu}_2\text{O}_3$  nanopowders. HUVEC. We detected almost no significant pro-angiogenic activity with  $\text{Eu}_2\text{O}_3$  nanopowders compared to  $\text{Eu}^{\text{III}}(\text{OH})_3$  nanorods (Figure 1d). These results indicate that our synthesized  $\text{Eu}^{\text{III}}(\text{OH})_3$  nanorods are capable of inducing better EC proliferation than commercially available  $\text{Eu}_2\text{O}_3$  nanopowders.

The fate of these nanorods in HUVEC was investigated after 24 h incubation using TEM, and internalization of nanorods inside the cytoplasmic compartments of the cells was observed (SI-Figure 2a–d). However, after internalization, the nanorods appeared like an amorphous material, which might be due to the low pH (~3.5) inside endoplasmic reticulum (ER), the organelle to which the nanorods are internalized. The mechanism of interaction of  $\text{Eu}^{\text{III}}(\text{OH})_3$  materials with HUVEC and their internalization inside the cytoplasmic compartment requires further investigation.

Our previous results demonstrated that the formation of reactive oxygen species (ROS), is a plausible mechanism by which inorganic nanorods induce angiogenesis <sup>5a</sup>. However it was not clear that which ROS are involved in angiogenesis by inorganic nanorods. In order to determine the role of ROS in endothelial cell proliferation, we have carried out a nanorod/VEGF (VF)-induced cell proliferation assay in the presence and absence of the antioxidant, *N*-acetyl-L-cysteine (NAC), which acts as an ROS scavenger (SI-Figure 3a–b). Before the use of NAC in HUVEC, we tested the cytotoxic effects of NAC on HUVEC at different concentrations (1–5 M). The data shows that beyond 2-M concentrations, NAC is toxic to

HUVEC (SI-Figure 3a). We observed the inhibition of nanorod-stimulated HUVEC cell proliferation at both concentrations (5  $\mu\text{g/mL}$  and 10  $\mu\text{g/mL}$ ) and inhibition of VEGF-stimulated cell proliferation in the presence 1 M NAC (SI-Figure 3b); however, we did not find complete inhibition of HUVEC cell proliferation. These results indicate the nanorods and VEGF induce EC proliferation in part via ROS formation.

It is well established that reactive oxygen species (ROS) play an important role in angiogenesis<sup>6</sup> by stimulating the key steps of cell proliferation, migration, and tube formation<sup>6a, 6d</sup>. In endothelial cells, especially, hydrogen peroxide ( $\text{H}_2\text{O}_2$ ) is the most biologically important ROS that is involved in redox signaling events during angiogenesis<sup>6</sup>(Figure 2.a). Earlier work found that in ECs, NADPH oxidase and xanthine oxidase are the major sources of intracellular ROS<sup>6a, 6d, 7</sup>. The generation of ROS derived from NADPH oxidase or xanthine oxidase, their interconversions from  $\text{H}_2\text{O}_2$  to water (in the presence of catalase) and  $\text{O}_2^{\bullet-}$  to  $\text{H}_2\text{O}_2$  (in the presence of SOD [superoxide dismutase]), and their role as a pro-angiogenic (e.g.,  $\text{O}_2^{\bullet-}$  and  $\text{H}_2\text{O}_2$ ) agent is shown schematically in Figure 2a. We therefore hypothesize that  $\text{Eu}^{\text{III}}(\text{OH})_3$  nanorods play an important role in the generation of ROS, especially hydrogen peroxide ( $\text{H}_2\text{O}_2$ ), which may be responsible for nanorod-mediated EC proliferation as well as in the *in vivo* zebrafish angiogenesis model system.

According to Figure 2a, the principle of dismutation of superoxide ( $\text{O}_2^{\bullet-}$ ) to hydrogen peroxide ( $\text{H}_2\text{O}_2$ ) by superoxide dismutase (SOD) and the decomposition of  $\text{H}_2\text{O}_2$  to water by catalase can be applied to nanorod-mediated HUVEC cell proliferation. It is known that the cell-permeable SOD mimetic, Mn(III) tetrakis(4-benzoic acid) porphyrin chloride (MnTBAP), catalyzes the dismutation of  $\text{O}_2^{\bullet-}$  to  $\text{H}_2\text{O}_2$  ( $k \approx 10^5 \text{ M}^{-1} \text{ s}^{-1}$ )<sup>8</sup> (Figure 2a). Therefore, it is essential to study the mechanism of nanorod-induced HUVEC proliferation in the presence and absence of MnTBAP (M) and catalase (C) to determine the role of ROS, such as  $\text{O}_2^{\bullet-}$  and  $\text{H}_2\text{O}_2$ , in cell proliferation (Figure 2b). This figure demonstrates that  $\text{Eu}^{\text{III}}(\text{OH})_3$  nanorods (Eu) alone promote 3.2-fold endothelial cell proliferation compared to untreated control cells. These results suggest that nanorods generate  $\text{H}_2\text{O}_2$ , which is responsible for HUVEC proliferation. There is no effect of catalase alone or MnTBAP alone on endothelial cell proliferation. However, when endothelial cells were incubated with  $\text{Eu}^{\text{III}}(\text{OH})_3$  nanorods (Eu) in the presence of MnTBAP (M), a surprising  $\sim 7$ -fold stimulation of HUVEC cell proliferation was observed. On the other hand, the experiment in the presence of catalase (C) shows an lesser of an increase in cell proliferation ( $\sim 2$ -fold stimulation) but higher than that of untreated control cells (Figure 2b). It might be assumed that there is no role for  $\text{O}_2^{\bullet-}$  in HUVEC cell proliferation in the presence of nanorods, as there is no inhibition of proliferation by MnTBAP. But formation of  $\text{O}_2^{\bullet-}$  by nanorods along with  $\text{H}_2\text{O}_2$  has a huge impact in the presence of M. There are two possibilities to explain the results obtained with M, namely (i) in the presence of  $\text{Eu}^{\text{III}}(\text{OH})_3$  nanorods (Eu), M generates a modified superoxide different from that which inhibits HUVEC cell proliferation, and treatment of catalase destroys this modified superoxide as well—that is, it has nothing to do with decomposition of hydrogen peroxide. This is an unlikely possibility, but one that cannot be excluded in the present experimental design; (ii) M (MnTBAP) catalyzes the dismutation of  $\text{O}_2^{\bullet-}$  to  $\text{H}_2\text{O}_2$ , which is highly responsible for angiogenesis<sup>6</sup>. Therefore, we hypothesize that initially,  $\text{Eu}^{\text{III}}(\text{OH})_3$  nanorods produce both  $\text{H}_2\text{O}_2$  and  $\text{O}_2^{\bullet-}$ , where  $\text{O}_2^{\bullet-}$  can be converted into  $\text{H}_2\text{O}_2$  in the presence MnTBAP. The cumulative production of  $\text{H}_2\text{O}_2$  (from nanorods alone and combined nanorods and MnTBAP) in the presence of M significantly increases HUVEC proliferation ( $\sim 7$ -fold stimulation, Figure 2b). These results provide evidence that ROS has a significant role in nanorod-mediated EC proliferation. However, factors other than formation of  $\text{H}_2\text{O}_2$  and  $\text{O}_2^{\bullet-}$  are still unknown and need further investigation.

In order to confirm our *in vitro* data in an *in vivo* system, we investigated the effects of M and nanorods in the (*fli1a:EGFP*) zebrafish embryos because of the optical transparency of the embryonic zebrafish and the availability of vascular-specific transgenic lines expressing green fluorescent protein (GFP). We injected Tris-EDTA solution as a vehicle (5 nl) (n=90), or MnTBAP (4.5 ng) (n=96), or Eu<sup>III</sup>(OH)<sub>3</sub> nanorod (50 ng) (n=90), or combined Eu<sup>III</sup>(OH)<sub>3</sub> nanorods(50 ng) and MnTBAP (4.5 ng) (n=85) (Figure 3a–d) at 48 hours post fertilization (hpf) in the perivitelline space [between the yolk and the periderm (duct of Cuvier area) and close to the developing subintestinal vessels] of Tg(*fli1a:EGFP*) embryos. The greatest numbers of embryos (65%) with ectopic blood vessels sprouting from SIV were observed in the embryos injected with the combination of nanorod and MnTBAP (Figure 3d). The nanorods alone showed ectopic sprouting in 37% of injected embryos (Figure 3c). MnTBAP-injected embryos showed ectopic SIV sprouting in 11% of the injected embryos (Figure 3b), which is close to the percentage for embryos injected with vector (TE) alone (9%, Figure 3a). The white stars indicate sprouts from the SIVs (Figure 3a–d). Figure 3e shows the number of embryos with ectopic sprouting from SIV resulting from each treatment. In summary, nanorods can potentiate angiogenic sprouting of SIV in zebrafish, and the pro-angiogenic effects of nanorods on zebrafish SIV are enhanced in the presence of MnTBAP. These results clearly support our *in vitro* data.

The exact composition of ROS formed by inorganic nanorods and their regulatory role in angiogenesis are not known. The formation of O<sub>2</sub><sup>•-</sup> in HUVEC has been measured by a standard HPLC method in which hydroethidium (HE) was used as a selective indicator of superoxide anion, whereas hydroxyl radical, singlet O<sub>2</sub>, H<sub>2</sub>O<sub>2</sub>, or nitrogen radicals were not detected<sup>9</sup>. The analysis of the cell lysate of HUVEC treated with VEGF (VF) as a positive control and different concentrations of nanorods using HPLC method shows a dose-dependent increase of superoxide anion with increasing concentrations of Eu<sup>III</sup>(OH)<sub>3</sub> nanorods (Figure 4). The mechanism of formation of the superoxide anion under these conditions is not fully understood. However, the present HPLC results clearly demonstrate the formation of superoxide anion in HUVEC in the presence of Eu<sup>III</sup>(OH)<sub>3</sub> nanorods (Figure 4).

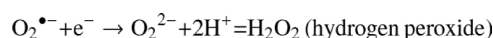
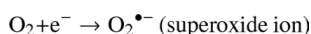
On the other hand, we investigated H<sub>2</sub>O<sub>2</sub> efflux generated from HUVEC in the presence of stimulation by VEGF or inorganic Eu(OH)<sub>3</sub> nanorods on a single-walled carbon nanotube (SWNT)/collagen sensor that is able to selectively detect H<sub>2</sub>O<sub>2</sub>, as demonstrated previously<sup>10</sup>. Thus, we applied this novel nanosensor platform<sup>10–11</sup> to the detection of H<sub>2</sub>O<sub>2</sub> efflux from HUVEC induced by angiogenic redox signaling in the presence of VEGF or Eu(OH)<sub>3</sub> nanorod stimulation, as shown in SI-Figure 4a–b. As shown in Figure 5a–f (cell image), the morphology of the cells stimulated with nanorods is the same as in the unstimulated cells, indicating that nanorods are not cytotoxic, as we reported before<sup>5a</sup>. Then one hundred individual SWNT sensors were selected, based upon their intensity ranking from highest to lowest, in order to calculate the number of stochastic transitions caused by H<sub>2</sub>O<sub>2</sub> using the previously described algorithm (Figure 5a–d). The location of each SWNT sensor underneath the cell was clearly verified by the nIR fluorescence image, which allows us to obtain the spatial information for H<sub>2</sub>O<sub>2</sub> generation from HUVEC<sup>12</sup>.

As shown in Figure 5a–d (spatial image), each SWNT sensor shows different numbers of transitions from 1–10, which indicates that the amount of H<sub>2</sub>O<sub>2</sub> generated from the cell stimulated by VEGF or nanorods varies at different locations. This spatial detection of H<sub>2</sub>O<sub>2</sub> at the single-cell level using the SWNT sensor is unique and might be useful in understanding the exact role of spatial orientation in the physiology and pathophysiology of angiogenesis. As shown in Figure 5e, the representative nIR fluorescence traces show a clear stochastic quenching response before and after stimulation, indicating the production of H<sub>2</sub>O<sub>2</sub> from HUVEC. As shown in the control trace (Figure 5e, Control), fluorescence

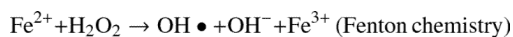
quenching was also observed even in unstimulated cells, which can be considered as a background signal of H<sub>2</sub>O<sub>2</sub> before stimulation. This background quenching can be attributed to H<sub>2</sub>O<sub>2</sub> production as a redox-signaling molecule in other physiological responses and also as a part of cell respiration. In this case, nitrogen oxides (NO<sub>x</sub>) have been implicated in the basal production of H<sub>2</sub>O<sub>2</sub> in the HUVEC membrane. Next we quantitatively compared the number of stochastic transitions for each stimulating condition to the background transduction. As shown in Figure 5f, the number of transitions per sensor for unstimulated cells is 0.7. After stimulation with VEGF, however, the number of transitions per sensor increased to 1.3, which is an almost two-fold increase compared to the control. This result clearly suggests that H<sub>2</sub>O<sub>2</sub> is generated much more for HUVEC stimulated by VEGF and diffuses out from the cell membrane, which allows the SWNT sensor to effectively detect it. However, the increase in the number of transitions is not observed in the case of cells stimulated by Eu(OH)<sub>3</sub> nanorods or even co-stimulated by both nanorods and MnTBAP (Figure 5f). This result suggests that the H<sub>2</sub>O<sub>2</sub> production mechanisms for VEGF and nanorod stimulation might be different. This hypothesis is supported by the intracellular detection of H<sub>2</sub>O<sub>2</sub> using an organic dye probe, as demonstrated previously<sup>5a</sup>. The intracellular production of H<sub>2</sub>O<sub>2</sub> increases for both VEGF and nanorod stimulation. Therefore, we conclude that the production of H<sub>2</sub>O<sub>2</sub> in angiogenic signaling in HUVEC increases after stimulation with both VEGF and Eu(OH)<sub>3</sub> nanorods, but it is generated near the cell membrane for VEGF and in the cytoplasm for nanorod stimulation.

The major objective of this research was to investigate the molecular mechanism of inorganic nanorod-mediated angiogenesis in endothelial cells (HUVEC). We have observed that Eu<sup>III</sup>(OH)<sub>3</sub> nanorods generate ROS, mainly H<sub>2</sub>O<sub>2</sub>, that regulate signal transduction pathways during angiogenesis. While Eu<sup>III</sup>(OH)<sub>3</sub> nanorods are not growth factors like vascular endothelial growth factor (VEGF) or basic fibroblast growth factor (b-FGF), they behave as pro-angiogenic agents. This study in HUVEC was carried out in nearly serum-free medium (0.1% FBS) and without antibiotics. We therefore hypothesized that Eu<sup>III</sup>(OH)<sub>3</sub> nanorods are the source responsible for formation of ROS, especially O<sub>2</sub><sup>•-</sup> and H<sub>2</sub>O<sub>2</sub>, which regulate angiogenesis. The HPLC and SWCNT results clearly indicate the generation of both O<sub>2</sub><sup>•-</sup> and H<sub>2</sub>O<sub>2</sub> in HUVEC in the presence of Eu<sup>III</sup>(OH)<sub>3</sub> nanorods. However, the exact mechanism for the formation of ROS from Eu<sup>III</sup>(OH)<sub>3</sub> nanorods is yet unknown and needs further investigation.

Our observations and earlier work suggests that in endothelial cells, NADPH oxidase and xanthine oxidase are the major sources of intracellular ROS<sup>6a, 6d, 7</sup>. ROS, such as superoxide anion (O<sub>2</sub><sup>•-</sup>) and hydrogen peroxide (H<sub>2</sub>O<sub>2</sub>), are produced primarily in cells as a by-product of normal cellular metabolism during the conversion of molecular oxygen (O<sub>2</sub>) to water (H<sub>2</sub>O) as follows<sup>13</sup>



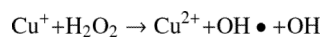
These ROS (O<sub>2</sub><sup>•-</sup>, and H<sub>2</sub>O<sub>2</sub>) are continuously formed in biological systems. However, this known chemistry does not provide any clear idea about the formation of ROS by inorganic nanorods [Eu(OH)<sub>3</sub>]. The earlier literature demonstrated the formation of ROS from metal ions as follows:



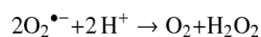
14



15

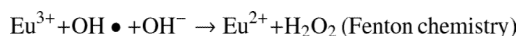


15

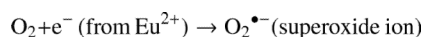


15

According to the above Fenton chemistry, we assume the following Fenton reaction where  $\text{Eu}^{\text{III}}(\text{OH})_3$  nanorods can generate  $\text{O}_2^{\bullet-}$  and  $\text{H}_2\text{O}_2$ :



16



It is reported that the trivalent europium ion ( $\text{Eu}^{3+}$ ) can be easily reduced to divalent europium ion ( $\text{Eu}^{2+}$ ) in certain conditions<sup>16-17</sup>. The mechanism by which  $\text{Eu}^{\text{III}}(\text{OH})_3$  nanorods can generate  $\text{O}_2^{\bullet-}$  and  $\text{H}_2\text{O}_2$  in biological systems needs rigorous investigation. However, the formation of ROS and detection of  $\text{H}_2\text{O}_2$  and  $\text{O}_2^{\bullet-}$  in HUVECs in the presence of nanorods was confirmed by single-walled carbon nanotube (SWNT) sensor and a HPLC method, respectively. According to earlier reports, the generation of ROS could be explained in two ways. Firstly, the metal ions (for example,  $\text{Fe}^{3+}/\text{Fe}^{2+}$ ,  $\text{Cu}^{2+}/\text{Cu}^{+1}$  etc.) can generate ROS in cellular metabolism using Fenton chemistry<sup>14-15</sup>. According to literature, inter-conversions of  $\text{Eu}(\text{III})$  to  $\text{Eu}(\text{II})$  or vice versa may occur at certain conditions<sup>16</sup>. Therefore, we speculated that the formation of ROS by  $\text{Eu}^{\text{III}}(\text{OH})_3$  nanorods in HUVECs may follow the Fenton chemistry (already discussed above). Secondly, the production of  $\text{O}_2^{\bullet-}$ , and  $\text{H}_2\text{O}_2$  levels are tightly controlled by several enzymes including catalase, glutathione peroxidase, thioredoxin, and peroxiredoxins<sup>18</sup>. Therefore, we can speculate that the inorganic nanorods could play an important role as an oxidant to directly inactivate PTP or phosphatase and tensin homolog (PTEN) in cytoplasm via oxidation of cysteine, which leads to mitochondrial  $\text{H}_2\text{O}_2$  production<sup>19</sup>. Apart from  $\text{Eu}^{\text{III}}(\text{OH})_3$  nanorods, other nanoparticles/nanorods can produce more or less ROS in biological system that need further study.

Considering the enormous application of angiogenesis by inorganic nanoparticles in biomedical nanotechnology, our long-term goal is to investigate in depth the regulatory pathways and role of  $\text{Eu}^{\text{III}}(\text{OH})_3$  nanorods along with group IV or III-V semiconductors or metals for angiogenesis study in future. In biological system, the group IV or III-V semiconductors or metals are responsible for the generation of less or more ROS that may or may not regulate signal transduction pathways during angiogenesis. In other way, the generation of ROS by group IV or III-V semiconductors or metals may be or may not be toxic to the cells. However, all these issues need further investigation. Again, this is a completely new area of research in the field of angiogenesis using inorganic nanorods. So far, we have not found a single report except carbon nanotubes<sup>4c</sup> and  $\text{Eu}^{\text{III}}(\text{OH})_3$  nanorods that indicates the angiogenesis study *in vitro* and *in vivo* model. The angiogenesis studies with nanoparticles of different morphologies are currently under investigation in our laboratory, which are beyond the scope of our present study.

Additionally, lanthanide-based inorganic nanoparticles, especially europium hydroxide nanorods, have attracted a great deal of attention in biology and medicine due to its fluorescence properties<sup>5c</sup> apart from pro-angiogenic properties. Hence, drugs or biomolecules attached to these nanorods can then be easily detected after internalization and benefit for future imaging, diagnostic and therapeutics purposes. In addition to fluorescence and pro-angiogenic properties of europium hydroxide nanorods<sup>5a</sup>, *in vivo* bio-toxicity and bio-availabilities of  $\text{Eu}^{\text{III}}(\text{OH})_3$  nanorods in mice models<sup>5b</sup> have been studied in a systematic way, that shows no biochemical and hematological toxicities. The present article also shows no toxicity in the zebra fish model after administration of  $\text{Eu}^{\text{III}}(\text{OH})_3$  nanorods. The non-toxic behavior of  $\text{Eu}^{\text{III}}(\text{OH})_3$  nanorods in mice and zebra fish model indicates that materials containing rare earths especially europium can be used in humans in future.

In summary, we have synthesized  $\text{Eu}^{\text{III}}(\text{OH})_3$  nanorods with an OH/Eu molar ratio of 4 that show excellent pro-angiogenic activity in *in vitro* and *in vivo* models at low concentrations. We have shown that the pro-angiogenic activity of  $\text{Eu}^{\text{III}}(\text{OH})_3$  nanorods in HUVEC is due to the formation of ROS, especially  $\text{H}_2\text{O}_2$ , the most biologically important ROS, which stimulate cell migration and proliferation, tube formation, and other processes.  $\text{Eu}^{\text{III}}(\text{OH})_3$  nanorods generate both  $\text{O}_2^{\bullet-}$  and  $\text{H}_2\text{O}_2$  in HUVEC. We have utilized a standard HPLC method for the determination of  $\text{O}_2^{\bullet-}$ . On the other hand, we have used a near-infrared fluorescent, single-walled carbon nanotube (SWNT) sensor array to measure the single-molecule efflux of  $\text{H}_2\text{O}_2$  from human umbilical vein endothelial cells (HUVEC) in response to pro-angiogenic factors. This result suggests that the mechanisms of  $\text{H}_2\text{O}_2$  production by VEGF or by nanorod stimulation are different. We have demonstrated that the production of  $\text{H}_2\text{O}_2$  for the angiogenic signaling in HUVEC increases after stimulation with both VEGF and  $\text{Eu}(\text{OH})_3$  nanorods, but it is generated near the cell membrane for VEGF and in the cytoplasm for nanorods. We have observed that nanorods alone can potentiate angiogenic sprouting of SIV in zebrafish but that the pro-angiogenic effects of nanorods on zebrafish SIV is enhanced in the presence of MnTBAP. This new study may provide the basis for the future development of new alternative therapeutic treatment strategies for diseases in which angiogenesis plays a significant role such as CVD, ischemic heart, limb diseases, and cancers.

## Supplementary Material

Refer to Web version on PubMed Central for supplementary material.



## Acknowledgments

This work was supported by National Institutes of Health (NIH) grant HL70567 and CA150190 and a generous gift from Bruce and Martha Atwater to DM; and the Ramanujan Fellowship grant (SR/S2/RJN-04/2010, GAP 0305\DST\CP) by DST, Govt. of India, New Delhi to CRP.

## References

1. (a) Folkman J. *Nature Medicine*. 1995; 1:27.(b) Risau W. *Nature*. 1997; 386:671. [PubMed: 9109485]
2. (a) Ferrara N, Gerber HP, LeCouter J. *Nature Medicine*. 2003; 9:669.(b) Basu S, Nagy JA, Pal S, Vasile E, Eckelhoefer IA, Bliss VS, Manseau EJ, Dasgupta PS, Dvorak HF, Mukhopadhyay D. *Nature Medicine*. 2001; 7:569.
3. Huston SL, Lengerich EJ, Conlisk E, Passaro K. *Jama-Journal of the American Medical Association*. 1999; 281:28.
4. (a) Claffey KP, Brown LF, delAguila LF, Tognazzi K, Yeo KT, Manseau EJ, Dvorak HF. *Cancer Research*. 1996; 56:172. [PubMed: 8548760] (b) Straume O, Akslen LA. *American Journal of Pathology*. 2002; 160:1009. [PubMed: 11891198] (c) Chaudhuri P, Harfouche R, Soni S, Hentschel DM, Sengupta S. Shape Effect of Carbon Nanovectors on Angiogenesis. *ACS Nano*. 2010; 4:574. [PubMed: 20043662]
5. (a) Patra CR, Bhattacharya R, Patra S, Vlahakis NE, Gabashvili A, Kolytyn Y, Gedanken A, Mukherjee P, Mukhopadhyay D. *Advanced Materials*. 2008; 20:753.(b) Patra CR, Moneim SSA, Wang E, Dutta S, Patra S, Eshed M, Mukherjee P, Gedanken A, Shah VH, Mukhopadhyay D. *Toxicology and Applied Pharmacology*. 2009; 240:88. [PubMed: 19616569] (c) Patra CR, Bhattacharya R, Patra S, Basu S, Mukherjee P, Mukhopadhyay D. *Clinical Chemistry*. 2007; 53:2029. [PubMed: 18035595]
6. (a) Lelkes PI, Hahn KL, Sukovich DA, Karmioli S, Schmidt DH. *Oxygen Transport to Tissue Xx*. 1998; 454:295.(b) Rhee SG. *Science*. 2006; 312:1882. [PubMed: 16809515] (c) Xia C, Meng Q, Liu LJ, Rojanasakul Y, Wang XR, Jiang BH. *Cancer Res*. 2007; 67:10823. [PubMed: 18006827] (d) Ushio-Fukai M. *Faseb Journal*. 2006; 20:A21.(e) Dardik R, Loscalzo J, Eskaraev R, Inbal A. *Arteriosclerosis Thrombosis and Vascular Biology*. 2005; 25:526.
7. (a) Lopez-Novoa JM. *Antioxidants & Redox Signaling*. 2002; 4:867.(b) Maulik N. *Antioxidants & Redox Signaling*. 2002; 4:783. [PubMed: 12470505] (c) Chen JP, Patil S, Seal S, McGinnis JF. *Nature Nanotechnology*. 2006; 1:142.
8. Huie RESP. *Free Radic Res Commun*. 1993; 18:195–99. [PubMed: 8396550]
9. (a) Bindokas VP, Jordan J, Lee CC, Miller RJ. *Journal of Neuroscience*. 1996; 16:1324. [PubMed: 8778284] (b) Rothe G, Valet G. *J Leukoc Biol*. 1990; 47:440. [PubMed: 2159514]
10. (a) Jin H, Heller DA, Kalbacova M, Kim JH, Zhang JQ, Boghossian AA, Maheshri N, Strano MS. *Nature Nanotechnology*. 2010; 5:302.(b) Jin H, Heller DA, Kim JH, Strano MS. *Nano Lett*. 2008; 8:4299. [PubMed: 19367966]
11. Cagnet L, Tsybouski DA, Rocha JDR, Doyle CD, Tour JM, Weisman RB. *Science*. 2007; 316:1465. [PubMed: 17556581]
12. Li QW, Zhang XF, DePaula RF, Zheng LX, Zhao YH, Stan L, Holesinger TG, Arendt PN, Peterson DE, Zhu YT. *Advanced Materials*. 2006; 18:3160.
13. (a) Katusic ZS. *Free Radical Biology and Medicine*. 1996; 20:443. [PubMed: 8720916] (b) Ames BN, Shigenaga MK, Hagen TM. *Proceedings of the National Academy of Sciences of the United States of America*. 1993; 90:7915. [PubMed: 8367443] (c) Zafarullah M, Li WQ, Sylvester J, Ahmad M. *Cellular and Molecular Life Sciences*. 2003; 60:6. [PubMed: 12613655]
14. Simm A, Brömmel HJ. *Signal Transduction*. 2005; 3:115.
15. Stohs SJ, Bagchi D. *Free Radical Biology and Medicine*. 1995; 18:321. [PubMed: 7744317]
16. Kuznetsov SA, Gaune-Escard M. *Electrochimica Acta*. 2001; 46:1101.
17. Casanova D, Bouzigues C, Nguyễn T-L, Ramodiharilafy RO, Bouzahir-Sima L, Gacoin T, Boilot J-P, Tharaux P-L, Alexandrou A. *Nature Nanotechnology*. 2009; 4:581.

18. (a) Suzuki YJ, Forman HJ, Sevanian A. *Free Radical Biology and Medicine*. 1997; 22:269. [PubMed: 8958153] (b) Veal EA, Findlay VJ, Day AM, Bozonet SM, Evans JM, Quinn J, Morgan BA. *Molecular Cell*. 2004; 15(1):129–139. [PubMed: 15225554] (c) Wood ZA, Schroder E, Harris JR, Poole LB. *Trends in Biochemical Sciences*. 2003;32. [PubMed: 12517450] (d) Zhao R, Holmgren A. *Journal of Biological Chemistry*. 2002; 277:39456. [PubMed: 12177067]
19. Connor KM, Subbaram S, Regan K-J, Nelson KK, Mazurkiewicz JE, Bartholomew PJ, Aplin AE, Tai Y-T, Aguirre-Ghiso J, Flores SC, Melendez JA. *J Biol Chem*. 2005; 280:1691.

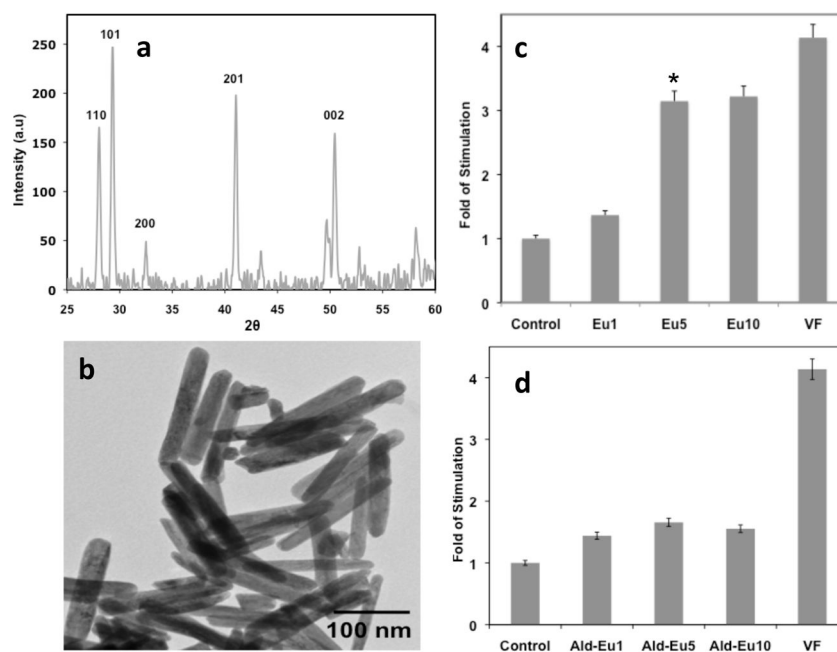


**Figure 1. (a–c). Physical characterizations of  $\text{Eu}^{\text{III}}(\text{OH})_3$  nanorods and the HUVEC cell proliferation assay**

(a) XRD phase analysis of as-synthesized  $\text{Eu}^{\text{III}}(\text{OH})_3$  nanorods, indicating that the product is purely crystalline. All reflections were distinctly indexed to a pure hexagonal phase of  $\text{Eu}^{\text{III}}(\text{OH})_3$  material. (b) TEM image of microwave-assisted as-synthesized  $\text{Eu}^{\text{III}}(\text{OH})_3$  nanorods obtained after 60 min of microwave heating, which clearly shows that the as-synthesized material consists entirely of nanorods with a diameter of 35–50 nm and a length of 200–300 nm. (c) HUVEC cell proliferation assay using radioactive [ $^3\text{H}$ ]-thymidine. The effect of europium hydroxide [ $\text{Eu}^{\text{III}}(\text{OH})_3$ ] nanorods at different concentrations (Eu-1, Eu-5, and Eu-10 indicates 1, 5, and 10  $\mu\text{g}/\text{ml}$ , respectively) in an endothelial cell proliferation assay is shown. VEGF (VF) was used as a positive control. (d) dose dependent effect of  $\text{Eu}_2\text{O}_3$  nanopowder obtained from Aldrich to HUVEC using cell proliferation assay [Ald-Eu-1, Ald-Eu-5, Ald-Eu-10 indicates 1, 5 and 10  $\mu\text{g}/\text{ml}$ ].

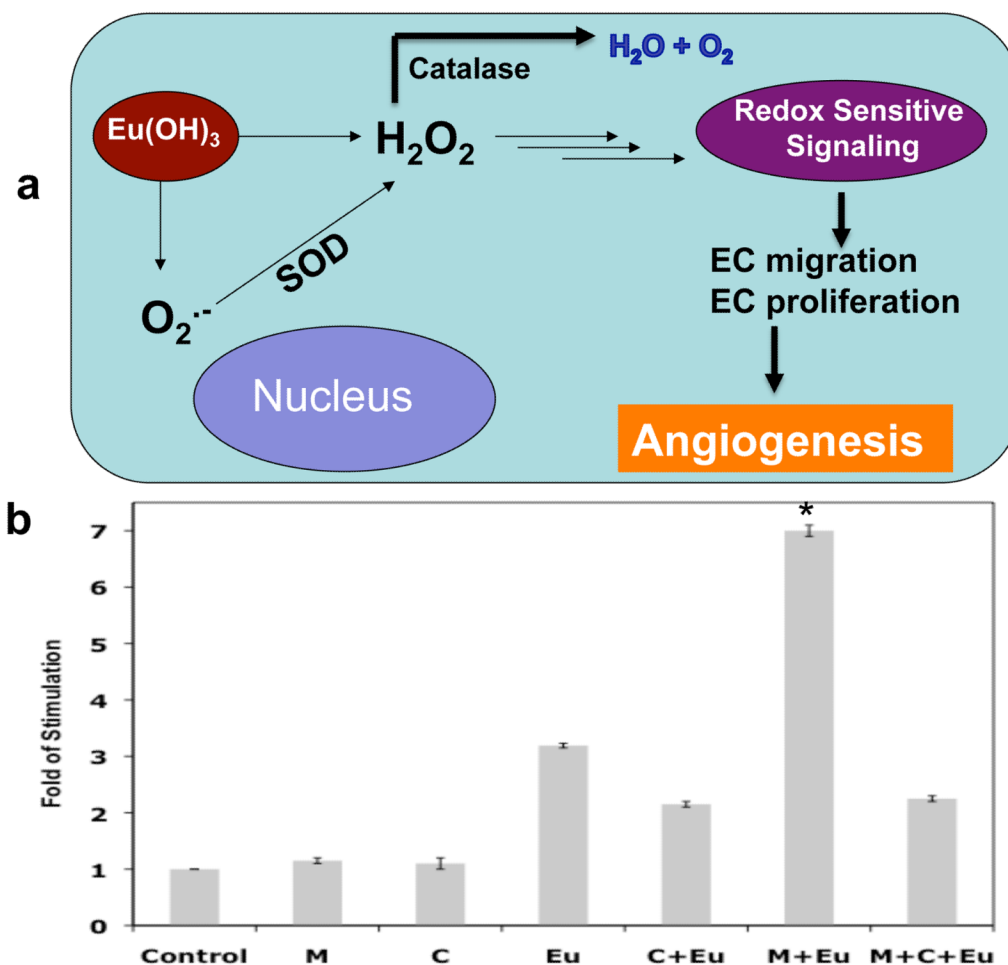


**Figure 2.** (a) **Redox signaling in angiogenesis by  $\text{Eu}(\text{OH})_3$  nanorods in endothelial cells (EC).** Generation of ROS, especially  $\text{H}_2\text{O}_2$  by  $\text{Eu}(\text{OH})_3$  nanorods, in the cytosolic part of the EC function as signaling molecules. (b) **HUVEC cell proliferation assay.** The effect of europium hydroxide [ $\text{Eu}^{\text{III}}(\text{OH})_3$ ] nanorod-induced HUVEC cell proliferation in the presence and absence of MnTBAP (SOD mimetic) and catalase was observed using radioactive thymidine- $\text{H}^3$ , with the results represented as fold stimulation. MnTBAP (10  $\mu\text{M}$ ) was incubated with cells in the presence or absence of nanorods and catalase in serum-starved EBM medium. Initially, MnTBAP (10  $\mu\text{M}$ ) was incubated with the cells for 15 minutes; then, catalase was added and the cells incubated for another 5 minutes; finally,  $\text{Eu}^{\text{III}}(\text{OH})_3$  nanorods (10  $\mu\text{g}/\text{mL}$ ) were added and the cells incubated for another 24 hours. After 24 hours, 1  $\mu\text{Ci}$  [ $^3\text{H}$ ]-thymidine was added into each well. Four hours later, the cells were washed with cold PBS, fixed with 100% cold methanol, and collected for the measurement of trichloroacetic acid-precipitable radioactivity. Experiments were performed in triplicate. C, catalase (1200 units/mL), M, MnTBAP (10  $\mu\text{M}$ ), Eu,  $\text{Eu}^{\text{III}}(\text{OH})_3$  (10  $\mu\text{g}/\text{mL}$ ). The data are statistically significant with  $p \leq 0.05$ . The mean  $\pm$  SD of three separate experiments, each performed in triplicate, was calculated.

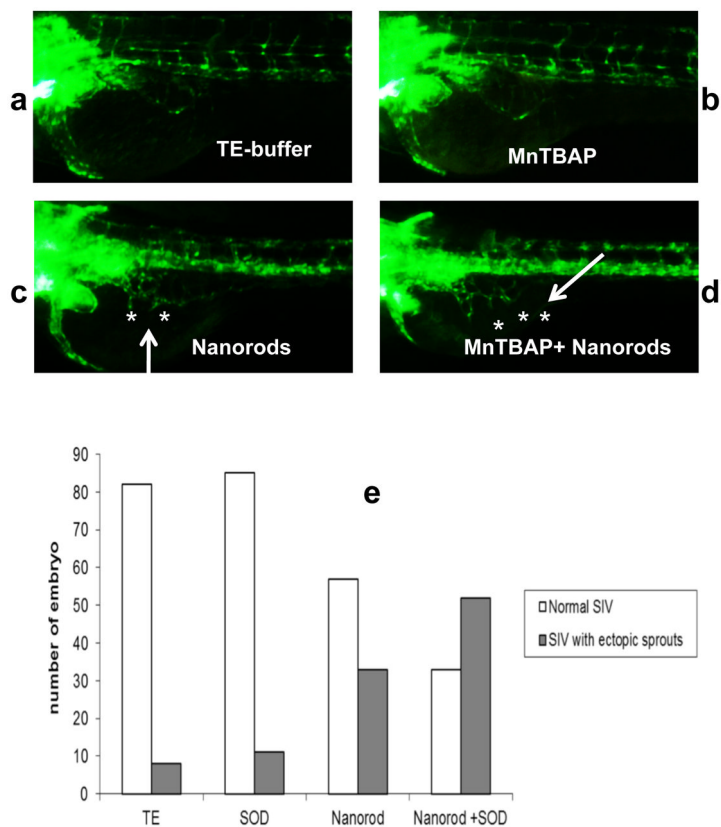


**Figure 3. (a–d).** *In vivo* angiogenesis study in a transgenic *FLI-1:EGFP* zebrafish model. Nanorods in combination with MntTBAP induce ectopic sprouting from the subintestinal vein (SIV): Lateral view of embryos at 72 hpf. The vehicle control was Tris-EDTA (TE), to which was added 4.5 ng of MntTBAP and/or 50 ng of nanorods. **(3e)** The number of embryos showing normal SIVs and ectopic sprouting from SIVs is summarized.

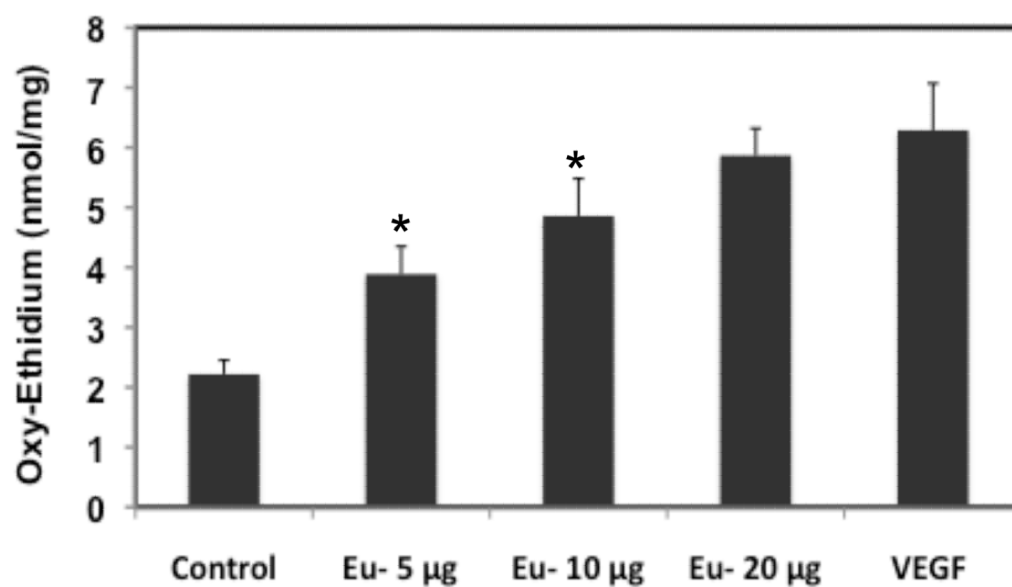


**Figure 4. Measurement of intracellular superoxide anion in HUVEC by an HPLC method using dihydroethidium**

HPLC identification of oxyethidium (nmol/mg) indicates the formation of  $O_2^{\bullet-}$  in HUVEC. HPLC samples were prepared and analyzed as described in Materials and Methods. The figure shows the intracellular  $O_2^{\bullet-}$  levels in HUVECs in the presence of different nanorod concentrations or stimulated by VEGF as a positive control.

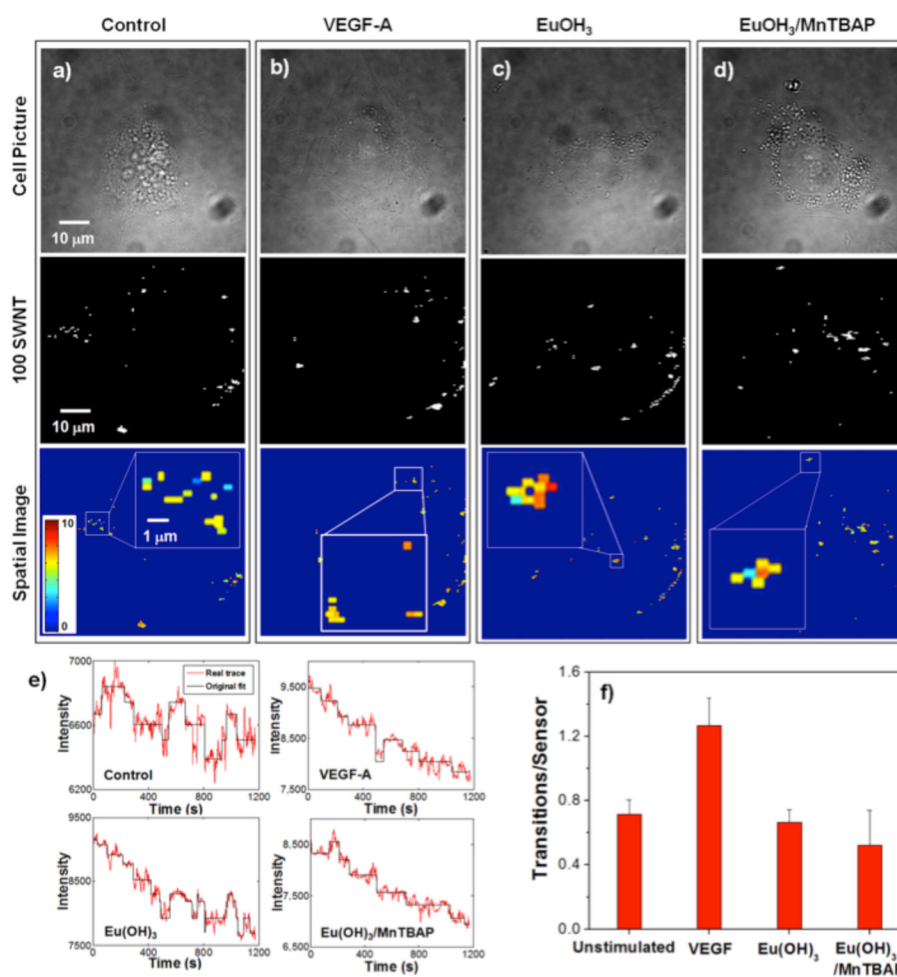


**Figure 5. Single-molecule detection of  $\text{H}_2\text{O}_2$  efflux from HUVEC with the SWNT/collagen sensor**  
**a)** Single-cell image, the location of 100 selected SWNT sensors, and a spatial image based on the number of stochastic transitions caused by  $\text{H}_2\text{O}_2$  efflux for unstimulated (control) cells; **b)** for VEGF-A; **c)** for  $\text{Eu}(\text{OH})_3$  nanorods; and **d)** for  $\text{Eu}(\text{OH})_3/\text{MnTBAP}$ . **e)** Representative traces of selected SWNT sensors underneath the unstimulated (control) cells, as well as VEGF-A-,  $\text{Eu}(\text{OH})_3$ -, and  $\text{Eu}(\text{OH})_3/\text{MnTBAP}$ -treated cells, showing the stochastic quenching response. **f)** The number of transitions per SWNT sensor measured for 20 min after stimulation.